

# Particle tracking simulation in the CSRe stochastic cooling system<sup>\*</sup>

HU Xue-Jing(胡雪静)<sup>1,2;1)</sup> YUAN You-Jin(原有进)<sup>1</sup> WU Jun-Xia(武军霞)<sup>1</sup>  
 ZHANG Xiao-Hu(张小虎)<sup>1,2</sup> JIA Huan(贾欢)<sup>1,2</sup>

<sup>1</sup> Institute of Modern Physics, Chinese Academy of Sciences, Lanzhou 730000, China

<sup>2</sup> University of Chinese Academy of Sciences, Beijing 100049, China

**Abstract:** A stochastic cooling system is under design and construction at HIRFL-CSRe (Heavy Ion Research Facility in Lanzhou - experimental Cooling Storage Ring), with the aim of cooling secondary particles produced at HIRFL-RIBLL2 (2nd Radioactive Ion Beam Line in Lanzhou). The optical layout of CSRe has been optimized to meet the requirements of a stochastic cooling system. In this paper, a particle tracking method is used to investigate both transverse and longitudinal cooling on the basis of the modified optical layout, demonstrating how it can be used to optimize stochastic cooling parameters. Simulation results indicate that the particle tracking method is an innovative and reasonable method to study stochastic cooling. It also has the advantage of discovering the influence of Twiss parameters at the pickups and kickers, which will be explored in further studies.

**Key words:** stochastic cooling, optical layout design, particle tracking, cooling rate

**PACS:** 29.20.D-, 29.20.dk, 29.30.Aj **DOI:** 10.1088/1674-1137/39/8/087001

## 1 Introduction

Beam cooling has the function of reducing the beam size and energy spread in a storage ring without beam loss [1]. Stochastic cooling was invented by Simon van der Meer, and this technique was widely studied at CERN (the European Organization for Nuclear Research) at the beginning of the 1970s. The goal of stochastic cooling is to decrease the energy spread and angular divergence of the beam. During the cooling process, the particles are ‘condensed’ and a finer beam with less energy spread and less angular divergence can be obtained [2].

Stochastic cooling is a feedback system. Transverse cooling uses a pickup electrode upstream to sense the transverse position error of the particle, and then this signal is amplified and applied to a kicker  $(2m+1)/4$  wavelength downstream. The kicker deflects the particle by an angle which is proportional to its displacement at the pickup [3]. Three methods are available for momentum cooling, namely Palmer cooling, notch filter cooling and time of flight cooling.

Palmer cooling uses a horizontal position pickup to measure the orbit displacement  $x_D = D \cdot \langle dp/p \rangle$  and the averaged momentum error of the sample in the meanwhile. However, there are other contributions to the

position error, especially the betatron oscillation  $x_\beta$  of the particles. Therefore, it is necessary to choose the focusing arrangement where  $x_D$  dominates over  $\langle x_\beta \rangle$ . The particle receives a ‘kick’ of momentum proportional to the detected displacement at the kicker [3].

Notch filter cooling utilizes a filter with a transmission minimum notch at each harmonic of the revolution frequency for longitudinal cooling. Particles with nominal energy will not experience any correction, while particles with a wrong revolution frequency will be accelerated or decelerated until all the particles have fallen into the notches. The price of filter cooling is that all the Schottky bands used have to be well separated, so it is ineffective to cool beams with high energy [4].

Time of flight (TOF) cooling uses the mixing from pickup to kicker to obtain the cooling signal. The notch filter is replaced by a 90° broadband phase shifter. Since there is no noise filtering function in the TOF system, small amplifier gain is inevitable to avoid the diffusion effect [5, 6].

The CSRe stochastic cooling system is mainly used to cool secondary particles coming from RIBLL2 (2nd Radioactive Ion Beam Line in Lanzhou), which is required for precise study of the decay properties of the radioactive ion beam (RIB) using the Schottky mass spectrometry (SMS) method [7]. Palmer cooling was chosen for

Received 13 February 2014, Revised 18 March 2015

<sup>\*</sup> Supported by Innovation Community of National Fund Committee (11221064) and National Key Basic Research and Development Project (2014CB845500)

1) E-mail: huxuejing@impcas.ac.cn

©2015 Chinese Physical Society and the Institute of High Energy Physics of the Chinese Academy of Sciences and the Institute of Modern Physics of the Chinese Academy of Sciences and IOP Publishing Ltd

longitudinal stochastic cooling because it has a larger momentum acceptance than filter cooling and allows larger amplifier gains compared with TOF cooling [6].

The particle tracking method is a new way of studying stochastic cooling, and is unlike other simulations published previously [8, 9]. During the turn-by-turn tracking of particles, stochastic cooling is realized simultaneously. By using this method, it is feasible to get the optimized cooling rate and cooling parameters. Transverse and longitudinal cooling are done simultaneously, and the cross influence of transversal and longitudinal cooling is also clear. Under different initial conditions, such as bandwidth, maximum input power and signal to noise ratio, cooling parameters like gain, cooling rate and mixing factor can be deduced for the optimal stochastic cooling design.

## 2 Design of optical layout for CSRe stochastic cooling system

CSRe is a specially designed heavy ion cooling storage ring with a circumference of 128.801 m [10]. The optical layout of CSRe is tailored for internal target experiments and high precision atomic mass measurements using stochastic cooling and electron cooling.

The equation of stochastic cooling rate  $1/\tau$  is given by [3]

$$\frac{1}{\tau} = \frac{W}{N} [2g(1-\tilde{M}^{-2}) - g^2(M+U)], \quad (1)$$

with optimum gain

$$g_{\text{opt}} = \frac{1-\tilde{M}^{-2}}{M+U}, \quad (2)$$

with the optimum cooling rate then given by

$$\frac{1}{\tau_{\text{opt}}} = \frac{2W}{N} \frac{(1-\tilde{M}^{-2})^2}{M+U}, \quad (3)$$

where  $W$  is the bandwidth,  $N$  is the particle number,  $M$  is the desired mixing factor from kicker to pickup,  $\tilde{M}$  is the undesired mixing factor from pickup to kicker and  $U$  is the noise to signal power ratio.  $g$  is the gain, which is defined as the fraction of observed sample error corrected per turn,  $-g = \Delta x / \langle x \rangle_s$  [3].

The maximum frequency of the cooling system has the form

$$f_{\text{max}} \leq \frac{1}{2T_{\text{pk}}|\eta dp/p|}. \quad (4)$$

where  $T_{\text{pk}}$  is the flight time from pickup to kicker,  $dp/p$  is the momentum spread, and the frequency slip factor is given by [11]

$$\eta = \frac{1}{\gamma_t^2} - \frac{1}{\gamma^2}, \quad (5)$$

where  $\gamma_t$  is transition gamma and  $\gamma$  the relativistic Lorentz factor.

Maximum frequencies of three different optical layouts ( $\gamma_t=1.395, 1.886, 2.629$ ) were calculated. The flight time  $T_{\text{pk}}$  from pickup to kicker was set to  $0.330 \mu\text{s}$  and the momentum spread  $dp/p$  was  $\pm 5 \times 10^{-3}$ . Results are shown in Fig. 1. Since the maximum magnet rigidity of CSRe is 9 Tm, the maximum energy is 708 MeV/u ( $^{12}\text{C}^{6+}$ ). Comparisons of acceptances among different modes in CSRe are listed in Table 1, with the acceptance of the stochastic cooling mode between the other two modes.  $\gamma_t$  was finally chosen close to 1.8 in order to get large maximum frequency  $f_{\text{max}}$ , keep the sign of eta  $\eta$  within the energy range between 400 MeV/u and 700 MeV/u, and maintain relatively large acceptance.

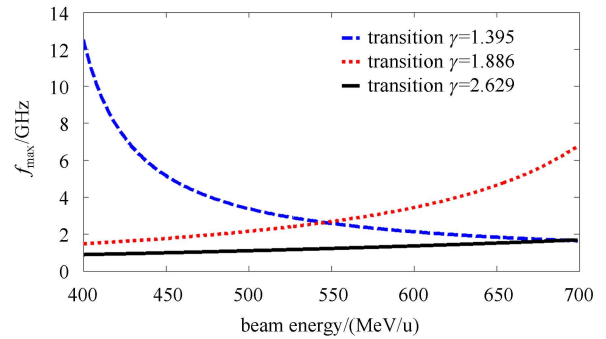


Fig. 1. (color online) Evolution of maximum frequencies is shown as a function of beam energy under different optical layouts of CSRe. Maximum frequency of the optical layout with transition gamma 1.886 is larger than that of the optical layout with higher gamma transition, but smaller than that with lower gamma transition.

The Twiss parameters of CSRe are shown in Fig. 2. Betatron tunes with different momentum spreads ( $dp/p=0, \pm 0.005, \pm 0.01$ ) are distributed within the area where only the 5th order resonance lines exist, as shown in Fig. 3. After chromaticity correction, betatron tune distribution can be narrowed to a smaller and stabler area.

Table 1. Acceptances of different optical layouts in CSRe.

	normal mode	stochastic cooling mode	isochronous mode
$\gamma_t$	2.629	1.886	1.395
$A_h/\pi\text{mm}\cdot\text{mrad}$	150 ( $dp/p=\pm 1.0\%$ )	130 ( $dp/p=\pm 0.5\%$ )	100 ( $dp/p=\pm 0.3\%$ )
$A_v/\pi\text{mm}\cdot\text{mrad}$	140	120	80

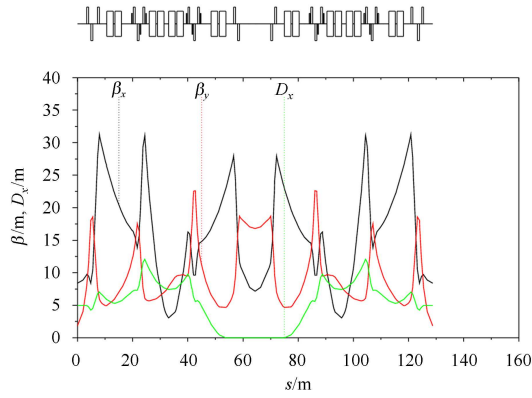


Fig. 2. (color online) CSRe twiss parameters are shown. Maximum  $\beta$ -function is 31.251 m in the horizontal direction and 22.612 m in the vertical direction. Maximum dispersion is 12.076 m, and the dispersion is 5.0 m at the target.

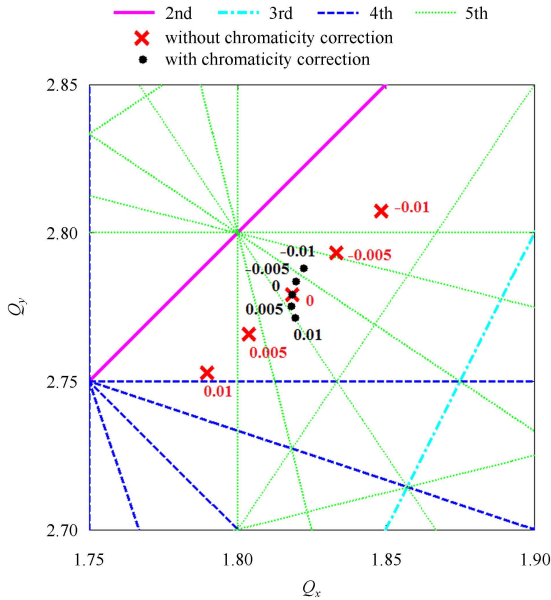


Fig. 3. (color online) Betatron tune distribution with different momentum spreads ( $dp/p = 0.01, 0.005, 0, -0.005, -0.01$ ) is shown, where the red crosses are the distributions before chromaticity correction and the black dots are those after chromaticity correction.

Since no spare space is available for the installation of pickups and kickers in CSRe, the electrodes are installed inside the dipoles [12]. In the designed optical layout, horizontal phase advance between dipole D15 and dipole D4 is  $88.74^\circ$ , and vertical phase advance between dipole D12 and dipole D3 is  $273.06^\circ$ , which is suitable for transverse stochastic cooling, as shown in Fig. 4.

The transverse displacement equation of single particle is [11]:

$$x(s) = a\sqrt{\beta_x(s)}\cos[\psi_x(s)+\xi_x]+D_x(s)dp/p, \quad (6)$$

where  $\psi_x(s)$  is defined as:

$$\psi_x(s) = \int_0^s ds/\beta_x(s), \quad (7)$$

$a$  and  $\xi_x$  are constants to be determined from initial conditions. Horizontal displacement consists of two components. By calculation of the beam parameters at the position of D12, displacement produced by dispersion was found to be relatively larger than that by  $\beta$ -function, so Palmer cooling was chosen here for longitudinal cooling. Detailed beam parameters at the positions of electrodes are shown in Table 2.  $\beta_x, \beta_y$  and  $D_x$  are the  $\beta$ -functions and dispersion respectively.  $A_x$  and  $A_y$  are the aperture limitations of the vacuum chamber.  $L_{pk}$  is the distance

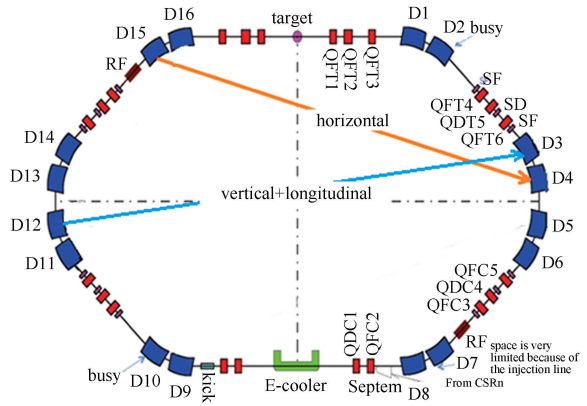


Fig. 4. (color online) Layout of CSRe stochastic cooling system. Horizontal electrodes are placed inside D15 and D4, and vertical and longitudinal electrodes are placed inside D12 and D3.

Table 2. Beam parameters for stochastic cooling in CSRe.

parameter	horizontal		vertical		longitudinal	
	pickup	kicker	pickup	kicker	pickup	kicker
$\beta_x/m$	22.027	4.723	3.068	12.270	3.068	12.270
$\beta_y/m$	6.075	6.977	7.916	5.755	7.916	5.755
$D_x/m$	5.307	7.679	7.423	8.651	7.423	8.651
$A_x/m$	0.110	0.110	0.110	0.110	0.110	0.110
$A_y/m$	0.035	0.035	0.035	0.035	0.035	0.035
$L_{pk}/m$	44.912		61.444		61.444	
$\theta/(\circ)$	88.74		273.06			

between pickup and kicker, and  $\theta$  is the phase advance between pickup and kicker.

### 3 Particle tracking method

In our particle tracking method, the bandwidth/pulse-length relation, known as the Küpfmüller or Nyquist theorem, is used. The time duration of a signal with a Fourier decomposition of bandwidth  $\Delta f=W$  is given by

$$T_s = \frac{1}{2W}. \quad (8)$$

A corollary to this theorem is applicable in transmitting short pulses. A short pulse passing a low pass or bandpass filter of bandwidth  $W$  will have a time width  $T_s$ , as shown in Eq. (8).

The theorem can also be applied directly to a stochastic cooling system. If a cooling system has a finite bandwidth  $W$ , then the kicker signal is a pulse of length  $T_s$  correspondingly. When a test particle passes the cooling system at  $t_0$ , it will be affected by all the particles that pass the cooling system from  $t_0 - T_s/2$  to  $t_0 + T_s/2$ . These particles are called to be part of the sample of the test particle. A uniform beam of length  $T$  (revolution time) can be sliced into  $T/T_s=2WT$  samples and particle number in each sample is averaged to  $N_s=N/(2WT)$  [3].

For every sample, its average position is detected by the pickup, and then corrected at the kicker. Due to the

momentum spread-induced difference in revolution time, particles are redistributed among samples turn by turn.

The particle signals detected by the pickup are very low, mainly depending on particle numbers and charge states. In order to generate enough power at the kicker, high power amplifiers are required. System noise such as the electronic noise and environmental noise will influence the cooling rate, which can be simulated by introducing an initial signal to noise ratio. Particles in three subspaces are assumed to experience the same noise level, which is assumed to keep constant during the cooling process.

### 4 CSRe stochastic cooling simulation and analysis

The parameters used in the particle tracking simulation are listed in Table 3. Evolution of emittances and momentum spread during  $3.5 \times 10^5$  turns is represented in Fig. 5. The cooling effect is obvious in the power-limited system within 1 kW. The horizontal cooling time constant is about 1.431 s, the vertical 1.298 s and the longitudinal 0.297 s from the tracking results.

The transverse aperture of the vacuum tube inside the bending magnets is 236 mm $\times$ 70 mm, and the electrodes will be installed inside the vacuum tube. The length of the electrode is about 2.76 m due to the limitation of the bending magnet. According to the Panofsky-Wenzel theorem, transverse kicks are only caused by the transverse gradient of the longitudinal field [13]. The

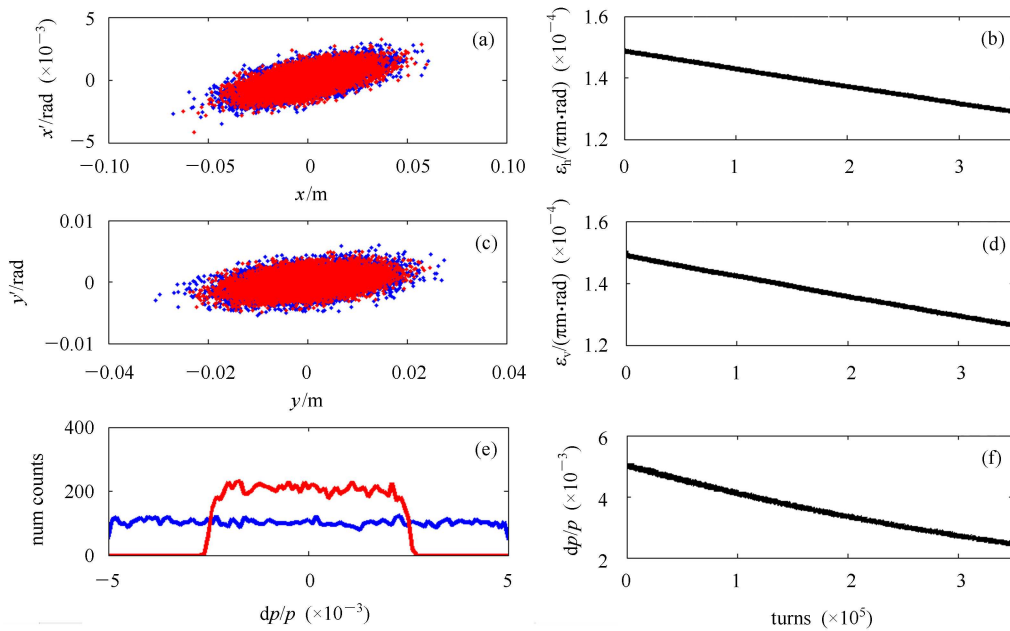


Fig. 5. (color online) Simulation results are shown for a power limit of 1 kW. (a) and (c) are the horizontal and vertical phase space evolutions respectively. (e) shows the momentum spread distribution. (blue: 1st turn; red:  $3.5 \times 10^5$ th turn). (b), (d) and (f) are the emittances and momentum spread tendencies during the  $3.5 \times 10^5$  turns.

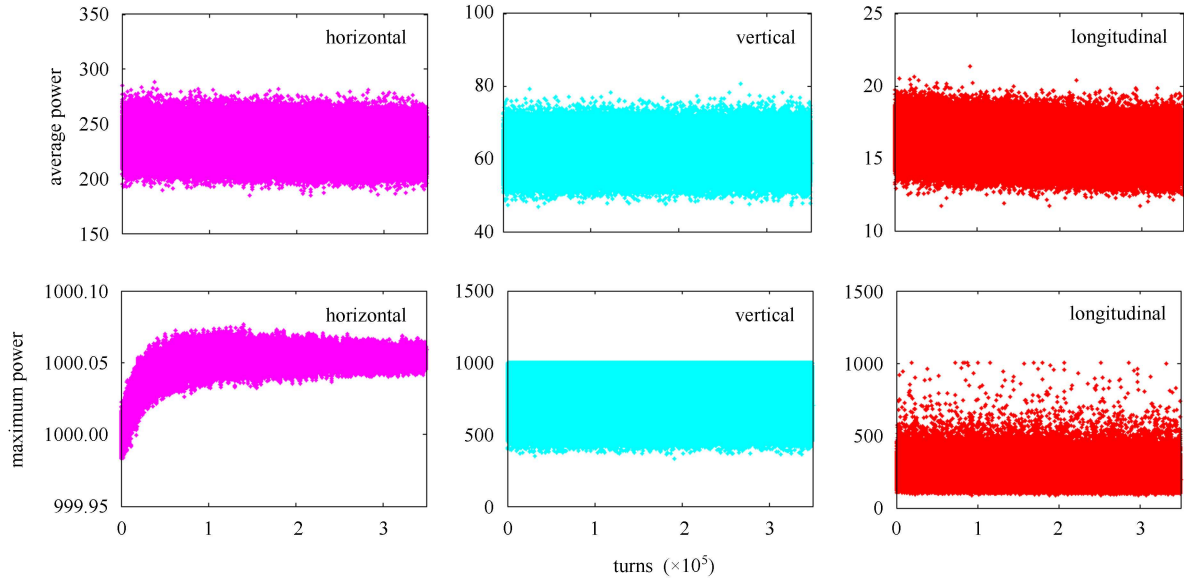


Fig. 6. (color online) Power during cooling process. Top: average power among samples during cooling in three subspaces. Bottom: maximum power among samples during cooling in three subspaces.

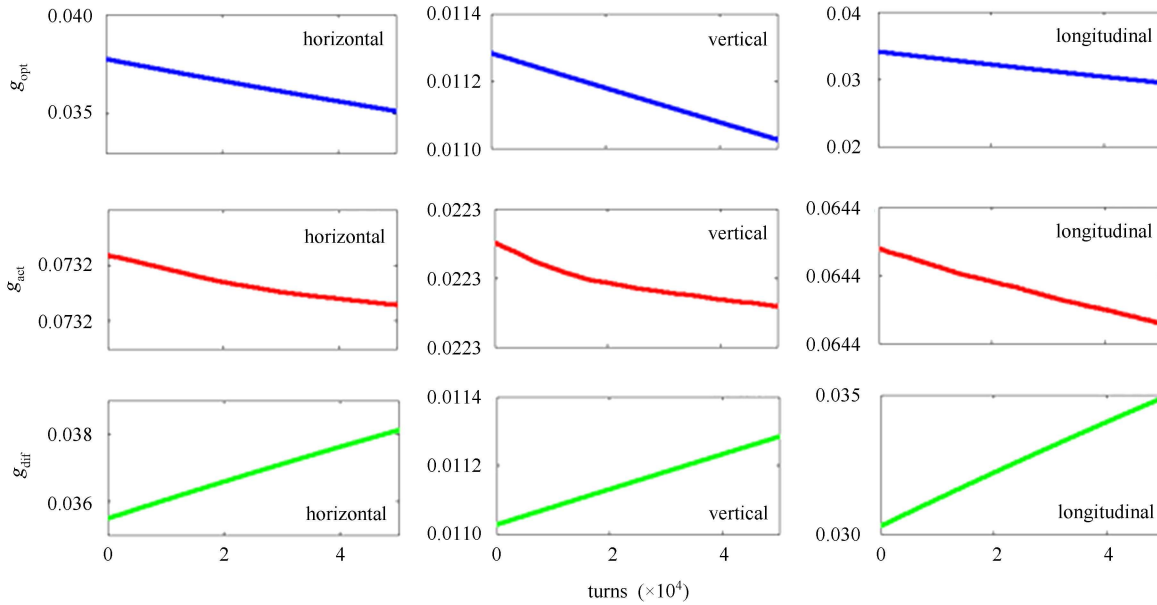


Fig. 7. (color online) Gain evolution. Top: optimum gain during cooling. Middle: actual gain during cooling. Bottom: difference between optimum and actual gain.

input power of the kickers needed for a transverse deflection angle  $\delta\Theta_{h,v}$  and a change of momentum spread  $\delta(dp/p)$  are represented as Eqs. (9) and (10) [13] respectively.

$$P_{h,v} = \frac{1}{2} \left( \frac{Am_0\beta^2c^2\gamma}{Ze} \right)^2 \frac{(nk_B b_{h,v})^2}{R_{s\parallel}} (\delta\Theta_{h,v})^2, \quad (9)$$

$$P_1 = \frac{1}{2} \left( \frac{Am_0\beta^2c^2\gamma}{Ze} \right)^2 \frac{1}{R_{s\parallel}} (\delta(dp/p))^2, \quad (10)$$

where  $A$  is mass number,  $Z$  is charge state,  $m_0$  is the atomic mass unit,  $c$  is the speed of light, and  $e$  is the elementary charge. The longitudinal shunt impedance  $R_{s\parallel}$  of the electrode in CSRe is  $640 \Omega$ , and  $k_B = \omega/\beta c$  is the beam wave number.  $2b_h$  and  $2b_v$  are the geometrical apertures of the vacuum tube inside the bending magnet in the transverse direction. Kicker is excited at the harmonic number  $n$  of the revolution frequency.

During the particle tracking process, particles in one

Table 3. Parameters of CSRe stochastic cooling simulation.

physical parameters	simulation data
beam kinetic energy, particle type	400 MeV/u, $^{12}\text{C}^{6+}$
$N$ (particle number)	10000
$2WT$ (sample number)	601
$\varepsilon_{h0}$ (initial horizontal emittance)	150 $\pi\text{mm}\cdot\text{mrad}$
$\varepsilon_{v0}$ (initial vertical emittance)	150 $\pi\text{mm}\cdot\text{mrad}$
$(dp/p)_0$ (initial momentum spread)	$\pm 0.005$
momentum cooling method	Palmer cooling
$W$ (frequency bandwidth)	500 MHz
$1/U_h$ (initial horizontal $S/N$ )	0.07
power limit	1 kW
CSRe circumference	128.801 m
$\gamma_t$	1.886
$N_{\text{pickup}}/N_{\text{kicker}}$	3/3

sample are assumed to experience the same input power as the kicker. Average power is defined as the averaged power over all the samples, and maximum power is defined as the maximum power among all the samples. The average power and maximum power used during cooling are shown in Fig. 6 for each subspace. In order to avoid heating in the cooling process, average power is much lower than maximum power.

In this paper, actual gain  $g_{\text{act}}$  was obtained by solving Eq. (1) and the cooling time constant was obtained from the evolution curve by using a fitting method. Optimum gain  $g_{\text{opt}}$  was obtained by Eq. (2), where the mixing factor and noise to signal ratio were obtained from the tracking results. During the particle tracking process, both the evolutions of the optimum gain  $g_{\text{opt}}$  and actual gain  $g_{\text{act}}$  have a tendency to decrease, but the difference  $g_{\text{dif}}$  between the two gains increases as the cooling pro-

ceeds, as shown in Fig. 7. Therefore, when the beam size is relatively large, better gain is obtained, which is closer to the optimum gain. It is therefore more efficient to cool a larger beam by stochastic cooling.

From Fig. 8, it is clear that below 1 kW, the cooling rate increases as the power increases. However, as the power limit continues to increase beyond 1 kW, the cooling rate stays almost constant instead of increasing correspondingly. Therefore, considering efficient use of power, it is unnecessary to increase the power limit.

Under the same power limit of 1 kW, comparisons of gain and cooling rate with different signal to noise ratios are represented in Fig. 9. It is obvious that larger gains are obtained with higher signal to noise ratios, while the cooling rates fall, unlike the gain evolution. Therefore, the optimum cooling rate should be achieved with a proper signal to noise ratio in the power-limited system.

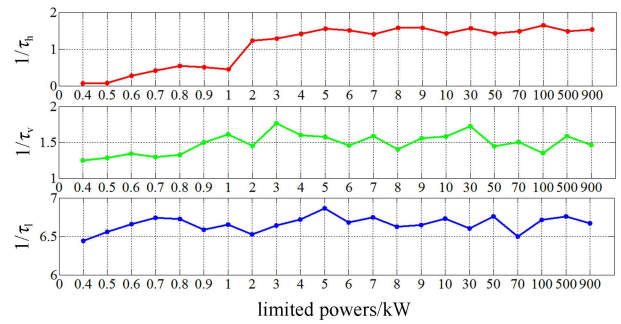


Fig. 8. (color online) Evolution of cooling rates  $1/\tau$  under different power limits in three subspaces. Cooling rates increase as the power limits increase up to 1 kW. When the power limit exceeds 1 kW, the cooling rate fluctuates around a constant.

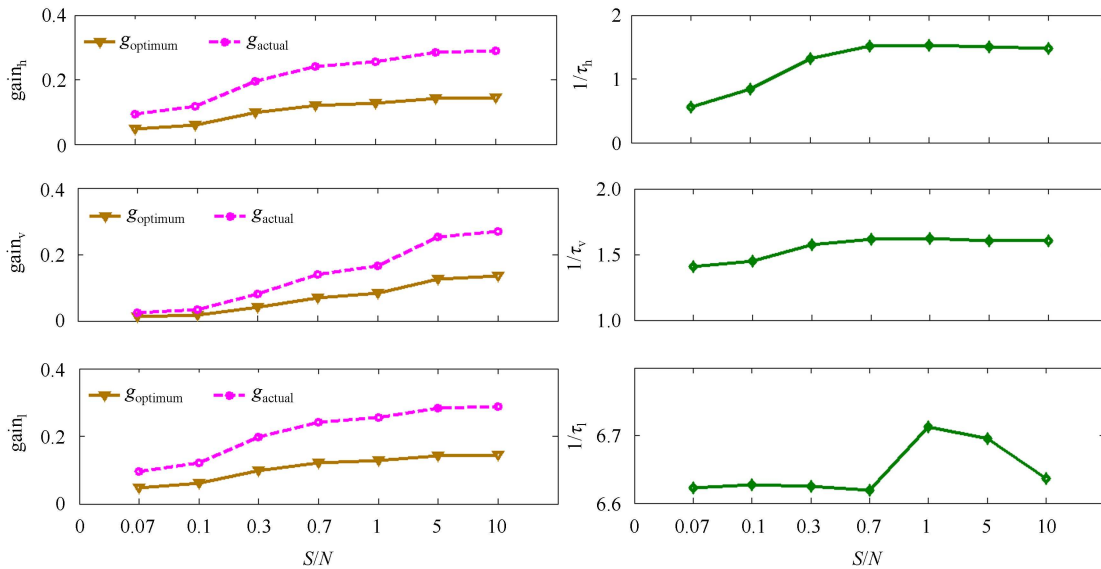


Fig. 9. (color online) Evolution of gain and cooling rate with different signal to noise ( $S/N$ ) ratios. Gain increases as the  $S/N$  increases, but the cooling rates reach a state of equilibrium or decrease as the  $S/N$  increases.

The above results were obtained under the same initial emittances and momentum spread. A comparison of situations with different initial transverse emittances and momentum spreads is shown in Table 4. By use of the particle tracking method, the cross influence of transversal and longitudinal cooling is clear.

Table 4. Cross influence between transversal and longitudinal cooling.

$\varepsilon_h/\varepsilon_v/dp/p$ ( $\pi\text{mm}\cdot\text{mrad}/(\pi\text{mm}\cdot\text{mrad})/(1)$ )	$\tau_h/s$	$\tau_v/s$	$\tau_l/s$
150/150/ $\pm 0.5\%$	1.431	1.298	0.297
150/100/ $\pm 0.5\%$	1.459	1.275	0.298
100/150/ $\pm 0.5\%$	1.371	1.285	0.298
150/150/ $\pm 0.2\%$	1.524	1.243	0.289
150/100/ $\pm 0.2\%$	1.499	1.259	0.291
100/150/ $\pm 0.2\%$	1.487	1.235	0.287

Figure 10 reveals the evolutions of signal to noise ratios during  $3.5 \times 10^5$  turns. The signal to noise ratio  $1/U$  has a tendency to decrease as the cooling proceeds. This is because the noise tends to remain the same, while the signal decreases as the beam shrinks.

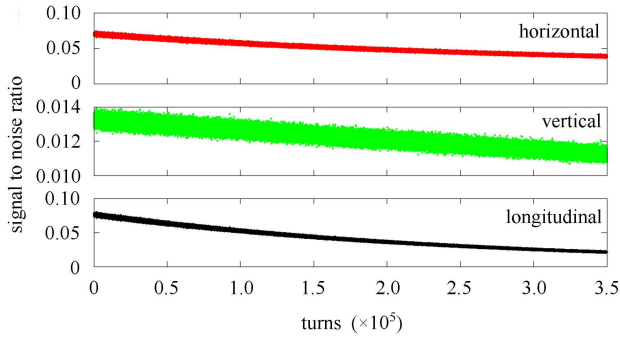


Fig. 10. (color online) Evolution of signal to noise ratios. The signal to noise ratios have a tendency to decrease as the cooling proceeds.

Due to the momentum spread, particles in one sample may move to other samples turn by turn. In the particle tracking simulation, the number of particles  $N_{\text{par}}$  that move away from their last sample and the number of samples  $N_{\text{sam}}$  that those particles  $N_{\text{par}}$  pass are counted. The mixing factor is defined as the ratio of  $N_{\text{sam}}$

to  $N_{\text{par}}$ .  $M_{\text{PK,KP}} = \Sigma((\Delta l - L_{\text{sample}}/2)/L_{\text{sample}})/\Sigma N_{\text{move}}$ , ( $|\Delta l| > L_{\text{sample}}/2$ ). For example, if the length of each sample is 0.336 m, and a particle moves 1 m away from its last staying sample after one turn, then the mixing factor of this particle is  $((1 - 0.336/2)/0.336)/1 = 2.476$ . Evolutions of mixing factors from pickup to kicker  $M_{\text{PK}}$  and from kicker to pickup  $M_{\text{KP}}$  in the transverse direction are shown in Fig. 11. Usually,  $M_{\text{KP}}$  is written as  $M^{-1}$ , and  $M_{\text{PK}}$  is written as  $\tilde{M}^{-1}$ . It is desirable that the mixing factor from kicker to pickup is larger than that from pickup to kicker.

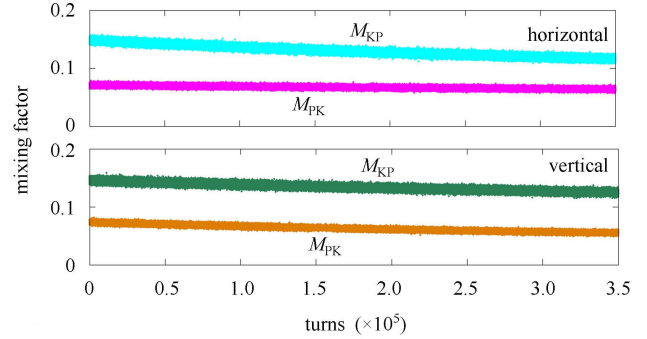


Fig. 11. (color online) Evolution of mixing factors.  $M_{\text{KP}}$  is larger than  $M_{\text{PK}}$ , which is desirable for better cooling.

As shown in Table 3, bandwidth is 500 MHz, initial particle number is 10000, and horizontal signal to noise ratio  $1/U_h$  is 0.07. If bandwidth, total particle number and  $1/U_h$  are changed, the results are as follows. Power was limited within 1 kW for all the situations.

Table 5 shows the cooling parameters under different initial conditions. It is possible to get a shorter cooling time with a wider bandwidth, smaller particle number and better signal to noise ratio.

## 5 Conclusion and outlook

The modified optical layout of CSRe meets the requirements of a stochastic cooling system. A stochastic cooling simulation has been demonstrated on the basis of the optimized optical layout.

Table 5. Comparison of cooling parameters under different initial cooling conditions.

$N$	$W$	$1/U_h$	$\tau_h/s$	$\tau_v/s$	$\tau_l/s$	loss rate (%)
10000	500 MHz	0.07	1.431	1.298	0.297	0.20
10000	1 GHz	0.07	0.869	0.661	0.154	0.21
5000	500 MHz	0.07	0.942	0.622	0.141	0.17
10000	500 MHz	0.7	1.300	1.246	0.300	0.19
10000	1 GHz	0.7	0.619	0.631	0.154	0.15
5000	500 MHz	0.7	0.615	0.583	0.140	0.21

Under different initial conditions such as input power of the kicker, signal to noise ratio, particle number and bandwidth, cooling parameters like cooling time, cooling rate, gain and mixing factor have been deduced in this paper.

Stochastic cooling has greater efficiency for cooling beams of larger size. It is easy to obtain a higher cooling rate when the power limit is relatively large, but increasing the power limit beyond a certain point is of no benefit in obtaining a higher cooling rate. In the power-limited system, optimum cooling rate is obtained with a proper signal to noise ratio. Shorter cooling times can be obtained with wider bandwidth, smaller number of particles and higher signal to noise ratio. A higher cooling rate is more likely when the signal to noise ratio is better, and thus it is important to decrease noise for better

stochastic cooling performance.

By using the particle tracking method, the cross influence of transversal and longitudinal cooling is apparent, which is hard to obtain through the Fokker-Planck equation or the basic equation of cooling rate. In further studies it should be feasible to discover the influence of Twiss parameters at the pickups and kickers.

Furthermore, the particle tracking simulation has succeeded in exploring space charge dynamics [14], and stochastic cooling of bunched ions simulation has also been successfully studied in the time domain [15].

In conclusion, the particle tracking method is an innovative and reasonable method to study stochastic cooling. Further simulations should be developed based on the particle tracking method, allowing more of its properties to become clear.

## References

- 1 Möhl D et al. Nuclear Instruments and Methods in Physics Research Section A: Accelerators, Spectrometers, Detectors and Associated Equipment, 2004, **532**: 1–10
- 2 <http://home.web.cern.ch/about/engineering/stochastic-cooling>
- 3 <http://cds.cern.ch/record/863007/files/p97.pdf>
- 4 Caspers F. Techniques of Stochastic cooling. In: European Organization for Nuclear Research CERN-PS Division. Physikzentrum Bad Honnef. Germany: Workshop on “Beam Cooling and Related Topics”, 2001. 1–17
- 5 Stockhorst H, Stassen R, Maier R et al. In: AIP Conference Proceedings, 2007, **950**: 239–255
- 6 Katayama T, Dimopoulou C, Dolinskii A et al. In: Proceedings of COOL 2013. Murren, Switzerland, 2013. 52–54
- 7 Schlitt B et al. Hyperfine Interactions. 1996, **99**: 117–125
- 8 WU Jun-Xia, XIA Jia-Wen, YANG Jian-Cheng et al. High Energy Physics and Nuclear Physics, 2004, **28**(3): 437–440 (in Chinese)
- 9 WU Jun-Xia, XIA Jia-Wen, YANG Jian-Cheng et al. High Energy Physics and Nuclear Physics, 2004, **28**(7): 767–770 (in Chinese)
- 10 XIA Jia-Wen et al. High Energy Physics and Nuclear Physics, 2006, **30**: 335–343 (in Chinese)
- 11 Lee S Y. Accelerator Physics. 2nd edition. Indiana University, USA: Fudanpress, 2006. 240–249
- 12 WU Jun-Xia. Research on CSR Stochastic Cooling (Ph. D. Thesis). Lanzhou: Institute of Modern Physics, CAS, 2005 (in Chinese)
- 13 Goldberg D A, Lambertson G R. Dynamic Devices. A Primer on Pickups and Kickers. In: The Physics of Particle Accelerators Vol. 1. AIP Conference Proceedings, Volume, 1992, **249**: 537–600
- 14 Holmes J A, Galambos J D, Blaskiewicz M et al. In: Conference Proceedings C980622, 1998. 1109–1111
- 15 Thorndahl L. In: Proceedings of COOL 2013. Murren, Switzerland, 2013. 49–51